A STUDY OF CONVECTIVE ELEMENTS IN THE ATMOSPHERIC SURFACE LAYER*

A. SHELBY FRISCH** and JOOST A. BUSINGER
Dept. of Atmospheric Sciences, University of Washington, Seattle, Wash. 98105, U.S.A.

(Received 1 May, 1972)

Abstract. A statistical model, based on a method of Vulf'son, is used to examine some of the plume-like temperature structures formed in the unstable boundary layer. The model assumes that the plume diameter changes slowly with height so that a cylindrical approximation may be made. Measurements of the vertical velocity and temperature were used to determine the temperature dependent portion of the vertical velocity field. Temperature data were collected from sensors on a tower and from aircraft; velocity data were collected only from the tower.

Using this model for analysis of the data indicates that: (1) the average isotherm diameter and the population of isotherms are a function of z/L; (2) the distribution of core temperatures is approximately a uniform distribution.

Independent of the model, a convective velocity was determined and found to have approximately the same profile as the temperature; from this the average velocity of the plumes was found to be a linear function of z/L, from $z/L \simeq 0.1$ to $z/L \simeq 1.0$. As a consequence of this functional dependence, the entrainment into the plumes is approximately constant over this range. The cumulative temperature distribution function was found to be an asymmetric function of z/L. A simple relation which is independent of u_* is given to determine the heat flux.

1. Introduction

At present considerable evidence exists that plume-like structures occur in the unstable atmospheric boundary layer. They are most easily observed when cold air flows over a warm water surface. In the resulting steam fog, many plumes may be observed if the wind is relatively light. Bryson (1955) analysed such a situation. Priestley (1956) used Woodcock's observations of gull patterns to obtain a qualitative idea of the convective structures as a function of the Richardson number. The coherence of temperature structures with height was first reported by Taylor (1958). This type of analysis was extended over greater heights by Kaimal and Haugen (1967) and in more detail by Kaimal and Businger (1970). Particularly striking evidence of plume-like structures has been obtained by McAllister *et al.* (1969) using an acoustic sounder.

On the basis of such evidence theoretical models of plumes have been developed, notably by Priestley and Ball (1955), Morton *et al.* (1956), Morton (1957), Turner (1963), and Telford (1966, 1970).

Since these isolated plume models are based on assumptions about the functional dependence of temperature, vertical velocity, entrainment and dissipation on the radial distance from the center, it appeared desirable to determine this dependence over an average of many convective elements. To do this realistically with measurements made in only one dimension (e.g., the level flight of an aircraft through the

* Contribution No. 269 Dept. of Atmospheric Sciences, University of Washington.
** Present address: Wave Propagation Laboratory, National Oceanic and Atmospheric Administration.

Boundary-Layer Meteorology **3** (1973) 301–328.

plume), it is necessary to make some assumptions about the geometry of the isotherms of the convective elements.

Vulf'son (1961), who was probably the first to examine this problem, assumed that the horizontal cross-sections of the plumes are circular. This assumption was somewhat substantiated by the studies of Chandra (1938), Woodward (1959), and others.

2. Method of Analysis

Define a field of elliptical shapes as shown in Figure 1, where the interior of the ellipse has a temperature $\theta' > \theta_{ref}$. This would exclude a 'cool' core, but would not exclude a hotter region with more than one element in the interior. For example, $\theta' \geqslant \theta_{ref} + k$ could be made up of two hotter elements contained in θ_{ref} as shown in Figure 2.

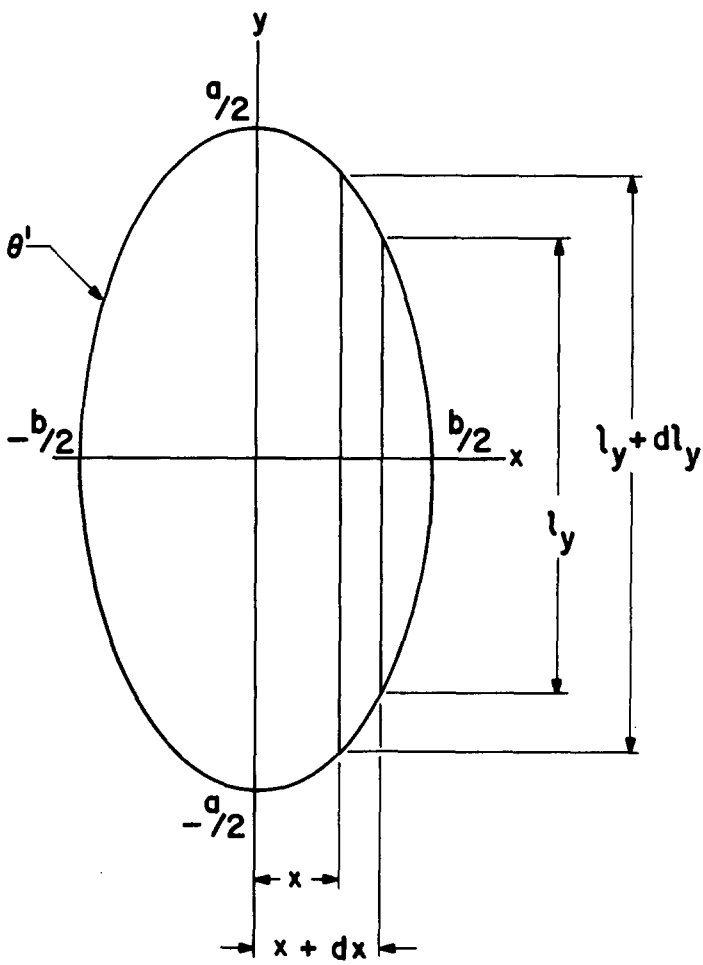

Fig. 1. Elliptical model of an isotherm with temperature θ', major and minor axis $a/2$ and $b/2$, respectively.

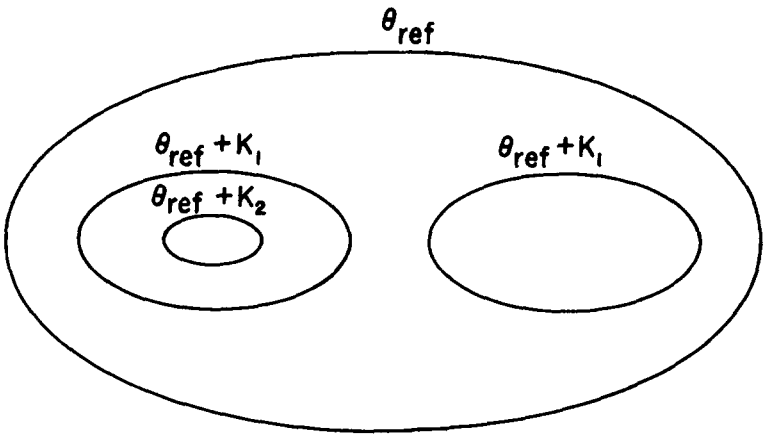

Fig. 2. Example of possible isotherms in the plume model.

Assume that the centers of the ellipses are uniformly distributed with an average of Nx centers along a unit edge in the x direction and Ny centers along the y direction. Let one of the axes be parallel to the mean wind which is along one of the coordinates. Define the density function describing the sets of elliptical axes by $f_{2,\theta'}(a)$ and $f_{1,\theta'}(b)$.

However, more recent evidence indicates that the shape of the cross-section of the plume is probably a function of stability, z/L, and that the circular cross-section occurs only under conditions approaching free convection, i.e., for $z/L \gg 1$. Therefore Vulf'son's statistical technique was generalized to include elliptical cross-sections of the plumes, where it was assumed that the plumes were elongated in the direction of the mean wind. Consequently it was assumed that all temperature fluctuations could be characterized by a population of isotherms of convective elements with elliptical cross-sections. The temperature fluctuation data were analyzed to give the number, size, and shape of the convective elements.

The study applied simultaneous measurements from aircraft and the Kansas tower which is equipped and run by the Boundary Layer Branch of the Air Force Cambridge Research Laboratories. The area, located near Liberal, Kansas, was flat farmland, with grain and other crops interspersed with occasional dry fields. The tower data provided reliable estimates of the fluxes, profiles and z/L. The aircraft provided temperature fluctuations along the path of flight, and the surface temperature.

In addition, the vertical velocity field was partitioned into a temperature and a non-temperature dependent part. This partition and the temperature distribution function were used to compute the vertical divergence of the upward moving air to estimate the inward flow into the plumes. These characteristics of the population were determined as functions of z/L. Finally, the similarity and plume profile assumptions of the models were compared with experimental results.

The use of the parameter z/L implies, of course, that it is assumed that the similarity theory of Obukhov (1946) is applicable to this study. Then $f_{2,\theta'}(a)$ and $f_{1,\theta'}(b)$ have

the following properties;

$$\int_0^\infty f_2(a)\,\mathrm{d}a = 1, \tag{1}$$

$$\int_0^\infty f_1(b)\,\mathrm{d}b = 1, \tag{2}$$

where the subscript θ' has been dropped for convenience. The average axis length is

$$\bar{a} = \int_0^\infty a f_2(a)\,\mathrm{d}a, \tag{3}$$

$$\bar{b} = \int_0^\infty b f_1(b)\,\mathrm{d}b. \tag{4}$$

In order to make the problem tractable we assume that:

$$a = m_0 b \tag{5}$$

for all a and b.

We define $W_{y,\theta'}(l_y \mid b)$ as the conditional probability density function for the chord lengths for $\theta' \geqslant \theta_{\text{ref}}$ in the y direction for an ellipse with axis b in the x direction as shown in Figure 1. Again for compactness, we drop the subscript for θ'. Since l_y is related to x, the conditional density may be written as

$$W_y(l_y \mid b) = f_y(x \mid b)\frac{\mathrm{d}}{\mathrm{d}l_y}(g \to x(l_y)), \tag{6}$$

where $f_y(x \mid b)$ is the conditional probability density of x taking a value along the axis b, and $g \to x(l_y)$ is the relation between x and l_y. Since the random variable x can take any value along b with equal probability,

$$f_y(x \mid b) = 2/b. \tag{7}$$

Now

$$x = b(\tfrac{1}{4} - y^2/a^2)^{1/2} \tag{8}$$

and also

$$y = l_y/2 \tag{9}$$

so

$$x = b/2(1 - l_y^2/a^2)^{1/2}. \tag{10}$$

Differentiating (10) with respect to l_y

$$\frac{\mathrm{d}x}{\mathrm{d}l_y} = \frac{bl_y}{2a^2}(1 - l_y^2/a^2)^{-1/2}. \tag{11}$$

Substituting this result and (6) into (5) yields

$$W_y(l_y \mid b) = \frac{l_y}{m_0 b}[(m_0 b)^2 - l_y^2]^{-1/2}. \tag{12}$$

Now

$$W_y(l_y \mid b)\, W_y(b) = W_y(l_y, b), \tag{13}$$

where $W_y(b)$ is the probability density function of the ellipses whose b axes are lying along a straight line.

This can be related to the density function, $f_1(b)$, of the b axes in the plane as follows: let the number of intersections per unit length in the y direction with ellipses whose axes have values from b and $b+\mathrm{d}b$ be

$$n(b)\,\mathrm{d}b = N_0 b f_1(b)\,\mathrm{d}b.$$

The total number of intersections per unit length is

$$n = N_0 \bar{b} \tag{14}$$

and the density distribution function of the b's measured along the direction parallel to the y direction is

$$W_y(b) = \frac{n(b)}{n} = \frac{b f_1(b)}{\bar{b}}. \tag{15}$$

Substituting this into (13)

$$W_y(l_y, b) = \frac{f_1(b)}{m_0 \bar{b}} \cdot l_y (m_0^2 b^2 - l_y^2)^{-1/2}. \tag{16}$$

What is measured, however, is the integral of all the population of the b's, i.e.,

$$W_y(l_y) = Re \int_0^\infty W_y(l_y, b)\,\mathrm{d}b. \tag{17}$$

Substituting (16) into (17),

$$W_y(l_y) = \frac{l_y}{m_0 b} \int_{l_y/m_0}^\infty f_1(b)\,\mathrm{d}b\,(m_0^2 b^2 - l_y^2)^{-1/2}. \tag{18}$$

The density function in the direction perpendicular to this can be determined in a similar manner. This function may be expressed as

$$W_x(l_x) = \frac{m_0^2 l_x}{\bar{a}} \int_{m_0 l_x}^\infty f_2(a)\,\mathrm{d}a\,(a^2 - m_0^2 l_x^2)^{-1/2}. \tag{19}$$

Since $a = m_0 b$,

$$f_1(b) = f_2(a(b)) \frac{\mathrm{d}a}{\mathrm{d}b} = m_0 f_2(a). \tag{20}$$

Thus the problem for describing the characteristics of the convective elements for any θ', is one of determining m_0 and either $f_{1,\theta'}(b)$ or $f_{2,\theta'}(a)$. Once this is determined, $N_{0,\theta'}$, the number of elements per unit area and the average area/unit element can be computed. The average axes length is

$$\bar{a} = \int_0^\infty a f_2(a)\,\mathrm{d}a \tag{21}$$

and the average area per element with temperature excess θ' may be expressed as

$$\bar{A} = \frac{\pi}{4}\overline{ab} = \frac{\pi}{4} m_0 \int_0^\infty a^2 f_2(a)\,\mathrm{d}a\,. \tag{22}$$

The total number of ellipses with a temperature excess θ' can be found by measuring the number of intersections $n_{\theta'}$, along a path of length L_x. Thus if the measurements were made in the x direction, the number per unit area is

$$N_{0,\theta'} = \frac{n_{\theta'}}{\bar{a} L_x}. \tag{23}$$

To compute a, a^2, and m_0 one may also determine moments of $w_x(l_x)$ and $w_y(l_y)$ for the ellipses in the same manner as Vulf'son did for circles. By definition we have

$$\overline{l_x^p} = \int_0^\infty l_x^p w_x(l_x)\,\mathrm{d}l_x\,. \tag{24}$$

Which after substituting (19) and changing the order of integration, can be integrated to

$$\overline{l_x^p} = \frac{1}{2m_0^p \bar{a}}\, a^{\overline{p+1}}\beta(p/2+1, \tfrac{1}{2}), \tag{25}$$

where $\beta(p/2+1, \frac{1}{2})$ is the Beta Function.
Similarly the moments of l_y may be determined:

$$\overline{l_y^p} = \tfrac{1}{2}\frac{m_0^p}{\bar{b}}\, b^{\overline{p+1}}\beta(p/2+1, \tfrac{1}{2}). \tag{26}$$

Since $a = m_0 b$,

$$a^{\overline{p+1}} = m_0^{p+1} b^{\overline{p+1}} \tag{27}$$

so $\overline{l_x^p}$ may be written as

$$\overline{l_x^p} = \frac{1}{2\bar{b}}\, b^{\overline{p+1}}\beta(p/2+1, \tfrac{1}{2}) \tag{28}$$

and letting $p=1$ for Equation (26) and (28) yields

$$m_0 = \bar{l}_y/\bar{l}_x . \tag{29}$$

To determine $\bar{a}$, let $p=-1$ in Equation (28)

$$\overline{l_x^{-1}} = \frac{m_0}{2\bar{a}}\beta\left(\tfrac{1}{2},\tfrac{1}{2}\right) = \frac{\pi}{2}\frac{m_0}{\bar{a}} \tag{30}$$

or

$$\bar{a} = \frac{\pi}{2}\frac{m_0}{\overline{l_x^{-1}}} . \tag{31}$$

The area of the average ellipse is determined by letting $p=1$ in Equation (25), thus

$$\overline{a^2} = \frac{4}{\pi} m_0 \bar{a} \bar{l}_x = 2m_0^2 \frac{\bar{l}_x}{\overline{l_x^{-1}}}$$

so by combining (22), and (31), and (27) the area $\bar{A}$ may be expressed as

$$\bar{A} = \frac{\pi}{2}\bar{a}\bar{b} = \frac{\pi}{2} m_0 \frac{\bar{l}_x}{\overline{l_x^{-1}}} . \tag{32}$$

An alternate way, and one which describes more completely the nature of the temperature structure, is to determine directly the probability density function $f_2(a)$ by solving the integral Equation (19). This type of Equation is known as an Abel Integral Equation.
Thus

$$w_x(l_x) = l_x \frac{m_0^2}{\bar{a}} \int_{m_0 l_x}^{a^*} f_2(a)\,(a^2 - m_0^2 l_x^2)^{-1/2}\,\mathrm{d}a , \tag{33}$$

where a^* is the upper bound of $f_2(a)$, i.e., $f_2(a)=0$ for $a \geqslant a^*$. Then using a method for solving the Abel integral equation, one may do the following:
let

$$m_0 l_x \equiv l$$

then

$$w_x(l_x) = w(l)\frac{\mathrm{d}l}{\mathrm{d}l_x} = m_0 w(l)$$

so Equation (33) may be written in terms of the new density function as

$$w(l) = \frac{1}{\bar{a}} \int_l^{a^*} f_2(a)\,(a^2 - l^2)^{-1/2}\,\mathrm{d}a . \tag{34}$$

Multiply by $(l^2 - q^2)^{-1/2}\,\mathrm{d}l$ and integrate from $l=q$ to $l=\infty$, after changing the order

of integration; we obtain

$$\int_q^\infty w(l)\,\mathrm{d}l\,(l^2-q^2)^{-1/2} = -\frac{\pi}{a}\int_q^{a^*} f(a)\,\mathrm{d}a. \tag{35}$$

Now, differentiate with respect to q

$$\frac{\mathrm{d}}{\mathrm{d}q}\int_q^\infty w(l)\,(l^2-q^2)^{-1/2}\,\mathrm{d}l = -\frac{\pi}{2\bar{a}}\frac{\mathrm{d}}{\mathrm{d}q}\int_q^{a^*} f(a)\,\mathrm{d}a = \frac{\pi}{2\bar{a}}f(q). \tag{36}$$

Thus

$$f(q) = \frac{2\bar{a}}{\pi}\frac{\mathrm{d}}{\mathrm{d}q}\int_q^\infty w(l)\,(l^2-q^2)^{-1/2}\,\mathrm{d}l. \tag{37}$$

The right-hand integral of (37) may be integrated by parts to

$$(l^2-q^2)^{+1/2}\frac{w(l)}{l}\Big|_q^\infty - \int_q^\infty (l^2-q^2)^{-1/2}\frac{\mathrm{d}}{\mathrm{d}l}\left[\frac{w(l)}{l}\right]\mathrm{d}l.$$

The first term vanishes on both upper and lower limits if $(l^2-q^2)^{1/2}\to\infty$ slower than $w(l)/l\to 0$, and since $f(a)=0$ for all $a\geqslant a^*$, $w(l)/l\to 0$ as $l\to\infty$ and finite m_0. Thus

$$\frac{\mathrm{d}}{\mathrm{d}q}\int_q^\infty w(l)\,(l^2-q^2)^{-1/2}\,\mathrm{d}l = \int_q^\infty q\,(l^2-q^2)^{-1/2}\cdot\frac{\mathrm{d}}{\mathrm{d}l}\left[\frac{w(l)}{l}\right]\mathrm{d}l.$$

Substituting this result into (37), the solution for $f_2(q)$ is

$$\frac{f_2(q)}{\bar{a}} = \frac{2}{\pi}q\int_q^\infty l\,(l^2-q^2)^{-1/2}\frac{\mathrm{d}}{\mathrm{d}l}\left[\frac{w(l)}{l}\right]\mathrm{d}l \tag{38}$$

and from (1)

$$\int_0^\infty \frac{f_2(q)}{\bar{a}}\,\mathrm{d}q = \frac{1}{\bar{a}}. \tag{39}$$

Solving Equation (38) requires a good estimate of $w(l)$ since the solution requires at least one differentiation of this function. In addition, the number of computations is much greater than the moment computation from the raw data. For these reasons, Equation (31) was used to determine $\bar{a}$.

3. Measurements and Data Reduction

The data used for the analysis were taken on 29 and 30 July, 1968 near Liberal, Kansas.

Aircraft data included air and surface temperature measurements obtained with a thermocouple and a PRT-5 radiometer, respectively.

The tower data which were made available by the Boundary Layer Branch of the Air Force Cambridge Research Laboratories included mean wind and temperature profile observations from 0.5–32 m as well as fluctuations of the three velocity components and the temperature at three heights (5.66 m, 11.3 m, and 22.6 m). A detailed description of the instrumentation is given by Haugen *et al.* (1971).

The results of the measurements from the aircraft and tower are interdependent; from the aircraft the elliptical constant, m_0, of the model was evaluated as well as other parameters of the model. For the tower calculations the estimates of m_0 determined from the airplane were used for the evaluation of the average size and number of elements at the lower levels.

In addition, tower measurements were used to determine gradients, Reynolds stress, heat flux, and vertical velocity structure for comparison purposes.

There were six values of z/L available from the tower for comparison of results. Measurements of θ' and w at 5.66, 11.32, and 22.64 m from the tower were used for the estimates of most of the statistical properties of the convective elements. The sampling rate was twice per second so that the minimum length scales resolved was about 2.5 m.

The Kansas Tower data used were taken from runs 28 and 40 for 1440 July 29, 1968 and 1034 July 30, 1968, respectively. An additional run, 41 taken at 1138 July 30, 1968 was also used for the estimation of the convective depth D. There were no profiles available for this run, however.

The aircraft data were divided into segments based upon the height and time of day. Those segments were subdivided as to direction and average difference between air and surface temperatures. Finally, only those parts of the subdivisions in which the surface temperature variations were less than 2 °C were used in the analysis, since much of the surface temperature data had variations of the order of 25 °C. After the corresponding air temperature data were filtered to remove low frequency trends, the average temperature for the particular subdivision was used as a reference level for the calculations. The data were sampled at every 0.1 s, giving a length resolution of about 5 m for the aircraft data.

Samples of the tower and aircraft data are shown in Figures 3 and 4. The average temperature is a few tenth's of a degree above the temperature base line. All estimates of w' were made by first computing $\bar{w}$ and subtracting this residual from each section used in the analysis.

The method used for the computations of the statistics at a given temperature level are shown in Figure 5. The $l_j(\theta')$'s were measured for the data sample and from these $l_j(\theta')$'s, $\overline{l^{-1}}(\theta')$ and $\bar{l}(\theta')$ were computed. The ratio of $\bar{l}(\theta')$ parallel and perpendicular to the wind was used to estimate the elliptical axis ratio; $m_0(\theta')$ (Equation (29)). Once m_0 was determined, Equation (30) and (5) were used to determine $\bar{a}(\theta')$ and $\bar{b}(\theta')$, in conjunction with the tower data. This was done by assuming Taylor's hy-

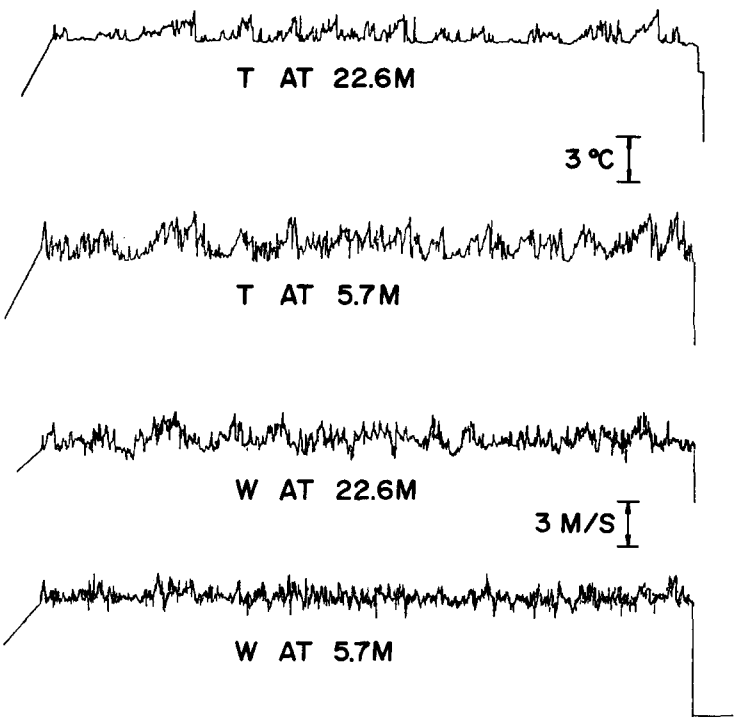

Fig. 3. Tower data sample of 7½ min for T and w at 5.7 m and 22.6 m heights.

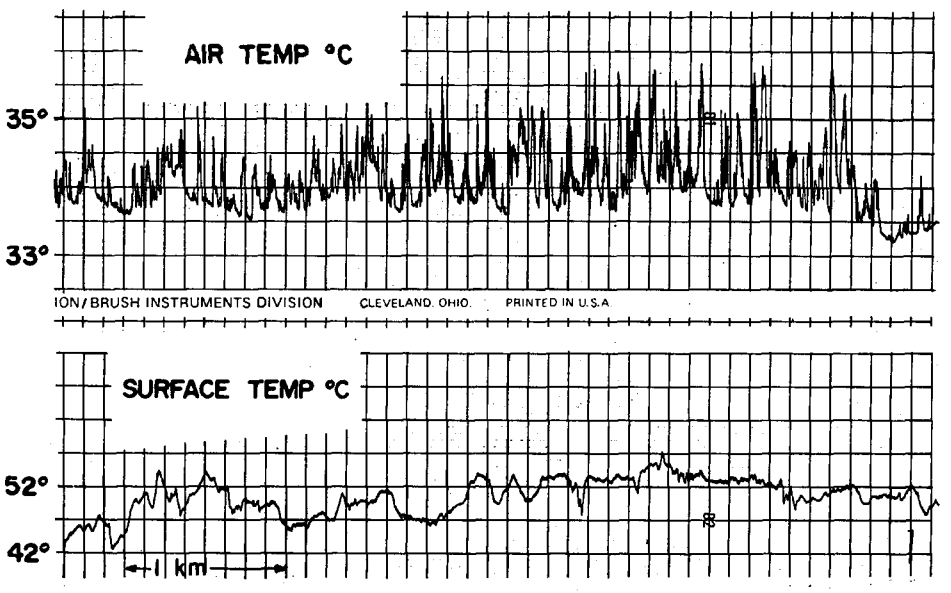

Fig. 4. Air and surface temperatures measured at 30 m (from aircraft).

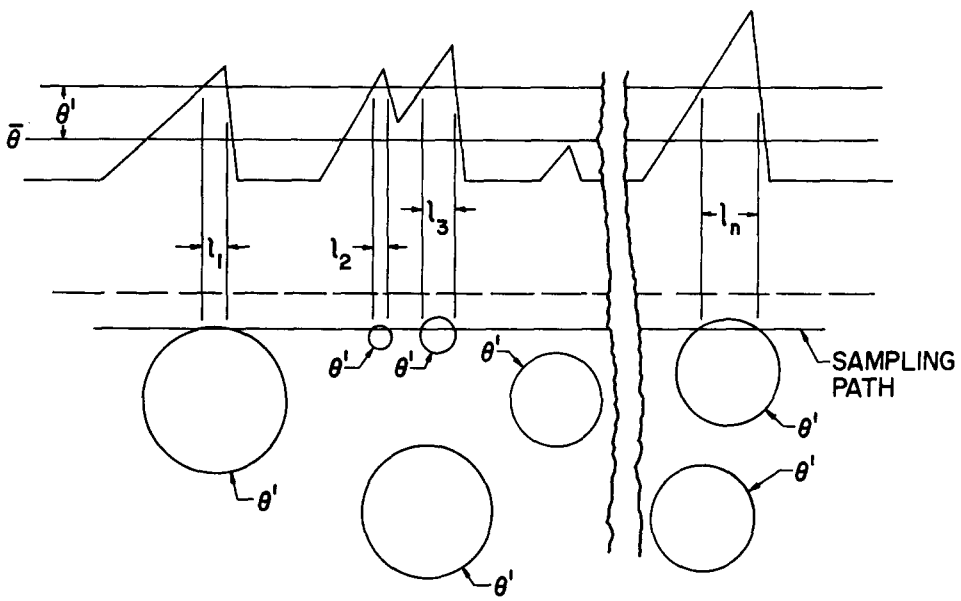

Fig. 5. Above: Simulated temperature trace with intersected length l_n at a temperature level θ'. Below: Representation of a random distribution of isotherms with temperature θ'. Measurement along the sampling path yields chord lengths l_n.

pothesis, i.e., $l = Ut$ where U is the mean wind speed at the level of measurement, and t is the time interval for a temperature greater than θ'.

The total number of $l_j(\theta')$'s per unit length, $n_0(\theta')$ was used to determine $N_0(\theta')$, the number of ellipses per unit area with temperature θ', by use of Equation (14) and the estimated value of $\bar{b}(\theta')$.

Table I summarizes the basic quantities obtained during runs 28 and 40. We use the approximation that $z/L = -Ri$ (Businger *et al.*, 1971). Note that the minus sign stems from our convention that L is positive in the unstable surface layer.

TABLE I

Basic parameters defining the surface layer for the analyzed runs

u^*	F_h	Height (m)	Ri	$N(0)$ (Number m^{-2})
		Run 28, 1440–1540 CDT, July 29, 1968		
31.4 cm s^{-1}	26.2 mW cm^{-2}	5.66	−0.399	5.8×10^{-3}
		11.32	−0.786	3.9×10^{-3}
		22.64	−1.20	2.9×10^{-3}
		Run 40, 1034–1134 CDT, July 30, 1968		
41.4 cm s^{-1}	20.3 mW cm^{-2}	5.66	−0.105	4.5×10^{-3}
		11.32	−0.303	2.9×10^{-3}
		22.64	−1.17	2.5×10^{-3}

4. Results

A. DETERMINATION OF m_0, THE AVERAGE PLUME DIAMETER $\bar{a}$ AND THE POPULATION OF ISOTHERMS N_0

A comparison of the first moments of l_x and l_y (Figure 6) measured from the aircraft indicates that the moments are approximately equal for $\theta' \geqslant 0$ within the accuracy of the analysis.

Thus

$$m_0 = 1; \quad \theta' > 0 \tag{40}$$

and

$$\bar{a}(\theta') = \bar{b}(\theta'); \quad \theta' > 0 \tag{41}$$

from Equation (5).

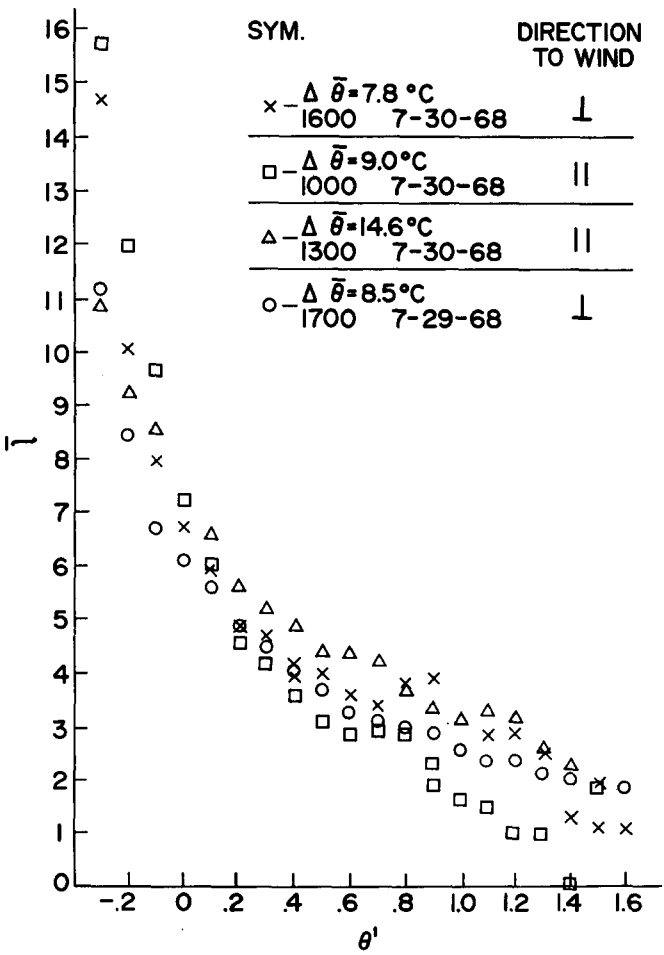

Fig. 6. Average relative chord length l as a function of temperature fluctuation θ' measured at 30 m from the aircraft. The $\overline{\Delta\theta}$ corresponds to the difference between the average surface and air temperature measured from the aircraft.

TABLE II

Plume characteristics

θ'	$z = 5.66$ m			$z = 11.32$ m			$z = 22.64$ m		
	$\bar{a}$(m)	$N \times 10^3$ m^{-2}	F	$\bar{a}$	$N \times 10^3$ m^{-2}	F	$\bar{a}$	$N \times 10^3$ m^{-2}	F
Run 28, (July 29 – 1440–1540)									
−0.6	12.1	3.8	0.33	13.6	2.3	0.31	16.3	1.1	0.25
−0.4	11.6	4.3	0.41	13.2	3.0	0.42	16.4	1.7	0.42
−0.2	10.2	5.4	0.49	14.3	2.9	0.50	14.6	2.3	0.51
0	9.6	5.8	0.56	11.4	3.9	0.57	12.7	2.9	0.61
0.2	9.5	5.5	0.62	10.5	4.1	0.65	11.7	3.0	0.69
0.4	9.2	5.1	0.63	9.6	4.1	0.71	13.1	2.3	0.76
0.6	8.9	4.6	0.73	9.8	3.6	0.77	11.7	2.1	0.81
0.8	8.8	4.3	0.78	10.1	3.2	0.82	10.5	2.3	0.85
1.0	9.2	3.7	0.82	9.5	2.9	0.85	10.1	1.9	0.89
1.2	7.9	4.2	0.85	8.5	2.9	0.88	8.6	2.0	0.91
1.4	7.5	3.9	0.88	8.5	2.8	0.90	9.3	1.5	0.93
1.6	7.3	3.5	0.90	8.5	2.0	0.93	9.4	1.1	0.95
1.8	6.8	3.2	0.93	7.4	1.9	0.95	7.3	1.3	0.97
2.0	6.6	2.6	0.94	7.6	1.8	0.97	5.2	1.1	0.98
2.2	6.1	2.4	0.96	6.8	1.0	0.98	5.7	0.4	0.99
2.4	5.6	1.8	0.97	6.0	0.7	0.99	6.1	0.2	0.99
2.6	6.7	1.0	0.98	5.9	0.6	0.993	9.6	0.1	0.995
2.8	5.0	0.9	0.99	3.0	0.4	0.996	0	0	1.0
3.0	4.4	0.5	0.992	0	0	1.0			
3.2	5.3	0.2	0.996						
Run 40, July 30 – 1034–1134									
−0.6	15.2	3.6	0.27	19.6	2.1	0.22	19.8	0.9	0.18
−0.4	13.5	4.6	0.36	17.5	2.8	0.33	25.1	1.4	0.30
−0.2	13.5	4.7	0.45	15.8	3.5	0.45	20.3	2.1	0.45
0	13.3	4.5	0.55	17.0	2.9	0.55	18.7	2.5	0.57
0.2	12.3	4.6	0.64	13.8	3.6	0.65	15.3	2.8	0.68
0.4	11.4	4.2	0.72	13.1	3.0	0.74	14.1	2.6	0.77
0.6	10.4	3.9	0.79	12.4	2.5	0.81	12.2	2.3	0.84
0.8	10.3	3.1	0.85	11.2	2.3	0.86	13.0	1.6	0.89
1.0	10.6	2.4	0.89	10.8	2.0	0.90	12.6	1.3	0.93
1.2	10.6	1.5	0.93	10.8	1.4	0.94	12.6	0.7	0.95
1.4	12.1	0.9	0.95	10.7	0.8	0.96	11.0	0.6	0.97
1.6	9.1	0.9	0.96	9.4	0.8	0.98	9.2	0.5	0.99
1.8	9.3	0.5	0.98	9.9	0.3	0.98	6.0	0.2	0.993
2.0	9.6	0.4	0.98	9.2	0.3	0.992	0.0	0	1.0
2.2	10.1	0.2	0.99	6.3	0.2	0.995			
2.4	5.0	0.2	0.994	0	0	1.0			
2.6	0	0	1.0						

However, examination of the data indicates that there may be a significant difference between the two directions for $\theta' < 0$, but the inhomogeneity of the surface temperature does not permit sample lengths of sufficient duration to determine the degree of this difference. Other investigators have noticed a difference in the cross-wind spectra of various components. Lenschow (1970) shows spectra of w for direc-

tions parallel and perpendicular to the wind at 100 m, with the prime difference being in the smaller wave-number range, with more energy appearing in the axis parallel to wind direction. Other investigators (McBean *et al.*, 1971 and Bean *et al.*, 1972) indicate similar results over the ocean.

It was assumed that our result from the aircraft data is also valid for the tower observations, so that the tower data could be used to determine the average isotherm diameter.

The average diameter appeared to be a function of height and stability. A careful analysis of the limited amount of data suggests that $\bar{a}$ is a logarithmic function of height and is proportional to $L^{1/3}$. This will be discussed further in the next section.

Knowing $\bar{a}$ and the fact that $m_0 \simeq 1$, the population of isotherms, $N(\theta')$ can be determined with Equations (14) and (41).

These results are given in Table II and form the basis for the following analysis.

B. THE 'ACCELERATION' DEPTH, D, AND DIMENSIONLESS ISOTHERMS AS A FUNCTION OF A DIMENSIONLESS PLUME DIAMETER

If one plots $N(0)$ vs. the logarithm of the height, two regimes may be distinguished. In the first or lower regime, N decreases with height and in the upper regime, N appears to become independent of height (Telford and Warner, 1967).

In the semi-logarithmic plot, the lower regime can be extrapolated to $N(0)=0$; the height at which this occurs is called 'the acceleration depth D' (see Figure 7). Surprisingly, D appears to be only weakly dependent on L, so that as a first approximation, D may be considered a constant independent of stability.

It should be pointed out that the acceleration depth has been derived only from the tower data. The aircraft observations at 30 m are in reasonable agreement with the upper level tower data but the aircraft observations at 100 m do not agree with the extrapolated dashed line of Figure 7. Clearly the number of plumes does not reduce to zero. Some plumes will extend to greater heights.

Because $\bar{a}$ is proportional to $L^{1/3}$ rather than L, another length scale is needed to form a dimensionless plume isotherm diameter. Such a scale is now provided for by D. The dimensionless form of the average plume diameter that seems best suited for correlation of the isotherms is

$$\bar{\varrho} \equiv \frac{\bar{a}}{D^{2/3}L^{1/3}}\left(\log_{10}\frac{D}{z} + 1.3\right). \tag{42}$$

The dimensionless form of the plume isotherms is given by

$$\eta = \theta'/\sigma_\theta .$$

This quantity is plotted as a function of $\bar{\varrho}$ in Figures 8 and 9 for measurements taken from the tower and the aircraft, respectively. The correlation is fairly good; the scatter of the points is about as small as can be hoped for.

The population of isotherms for the tower was made nondimensional by comparison with $N(0)$, i.e., Pop. $= N(\theta'/\sigma_\theta)/N(0)$. The results from the tower data are shown in

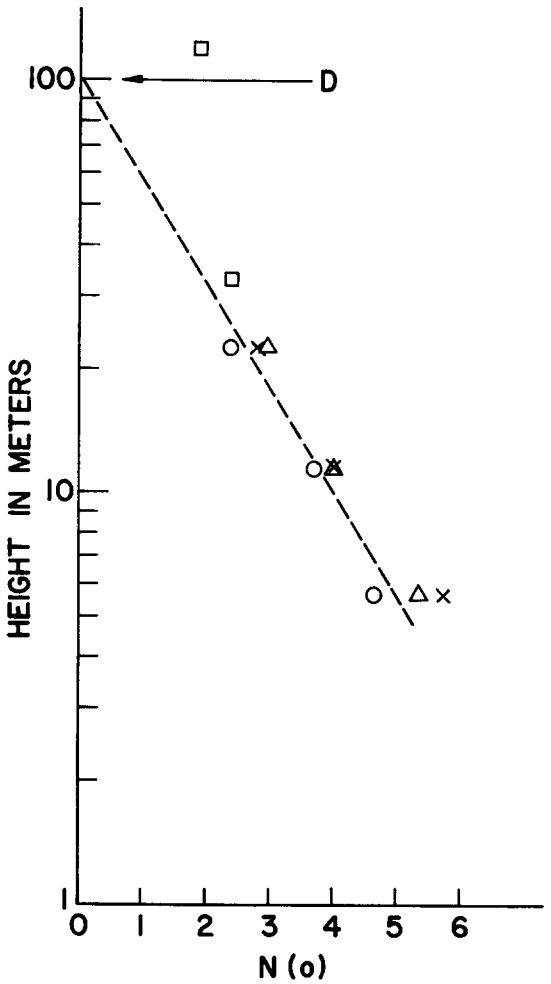

Fig. 7. Determination of D from $N_0(0)$, where the symbols ○, ×, △ are for the tower measurements, and □ for the aircraft measurements.

Figure 10. A comparison of the aircraft results is shown in Figure 11, again as a function of η.

C. CUMULATIVE TEMPERATURE DISTRIBUTION AND DETERMINATION OF THE PLUME BOUNDARIES

The cumulative temperature distribution function $F(\eta)$ was determined in terms of $\eta = \theta'/\sigma_\theta$.

It is defined by

$$F(\eta) = \int_{-\infty}^{\eta} p(\eta')\, \mathrm{d}\eta',$$

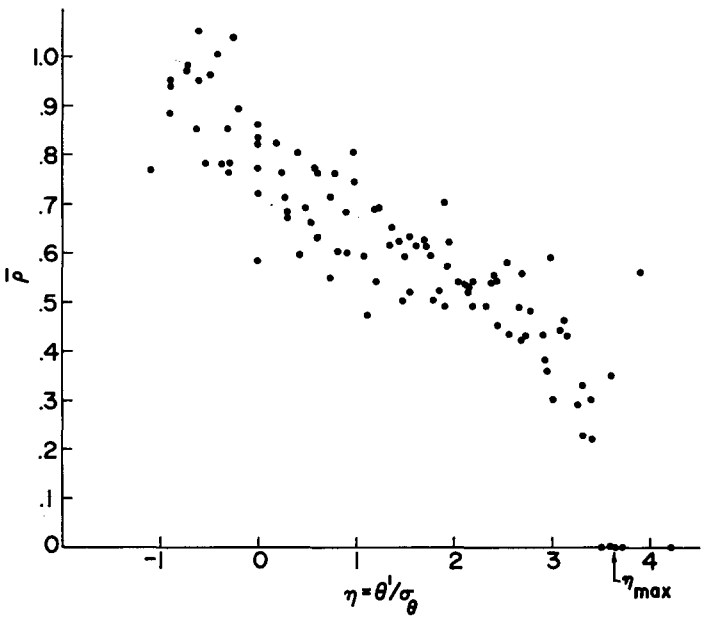

Fig. 8. Average non-dimensional plume radius as a function of the dimensionless temperature η measured from the tower.

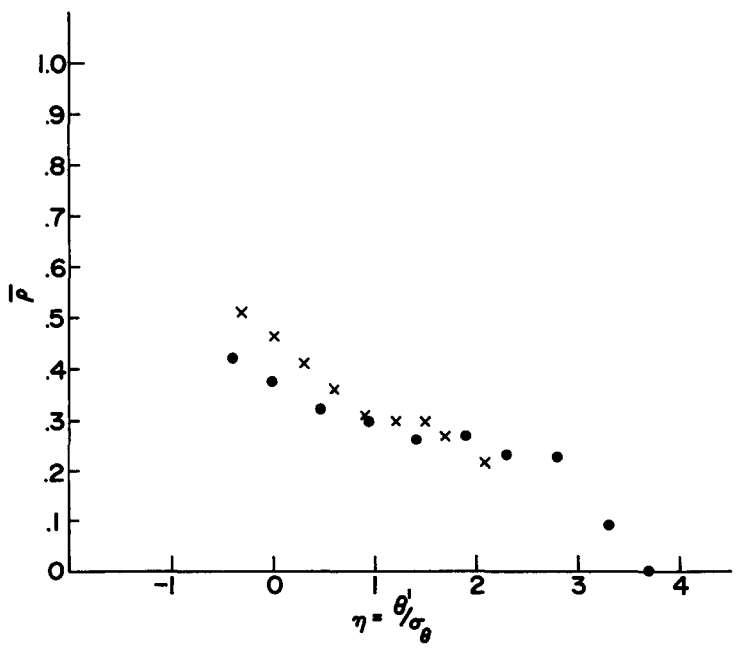

Fig. 9. Average non-dimensional plume radius as a function of the dimensionless temperature η measured from the aircraft.

which indicates the fraction of time that $\eta' \leqslant n$; $p(\eta)$ is the probability density function of η.

The result is plotted in Figure 12. As indicated by the two lines on the diagram, there are apparently two distinct distributions; one for $\eta < 0$ and one for $\eta > 0$. Similar results have been presented by Lenschow (1970) and Bean *et al.*, (1972). They also find two slopes for $F(\eta)$ with the transition at $\eta = 0$. If $\eta = 0$ corresponds with the boundary of the plumes, which we will verify in the following analysis, then this result indicates that the temperature variance inside the plume is greater than outside, a result which was expected from inspecting the temperature traces.

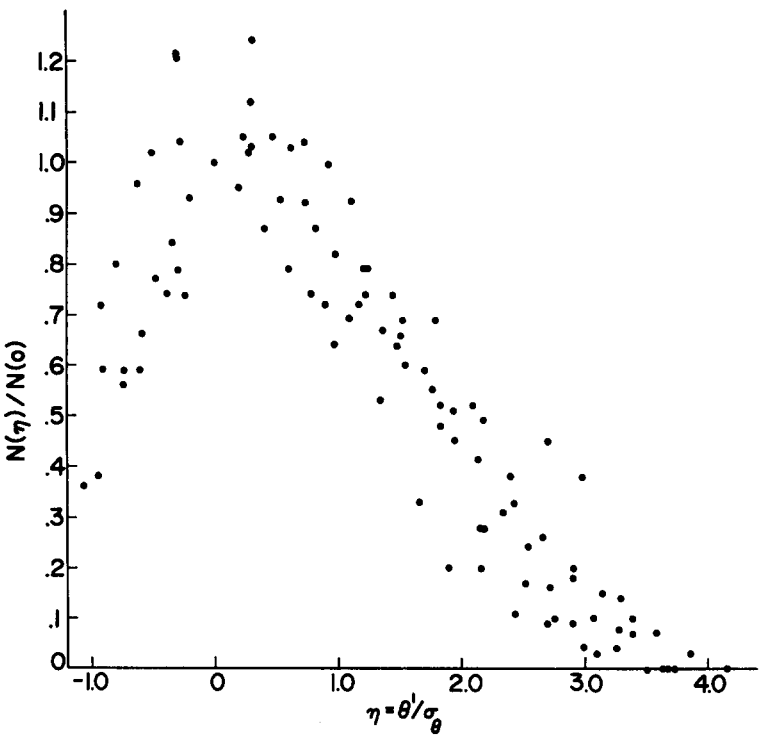

Fig. 10. Normalized population of isotherms as a function of the dimensionless temperature, η as measured from the tower. The normalization is the population at $\eta = 0$.

In order to determine what value of η corresponds to the boundary of the plumes, the conditionally expected value of the vertical velocity for given θ', $E(w \mid \theta')$, was computed for the two runs.

This was done by averaging w during the time θ' was in an interval from $\theta' - \Delta\theta'/2$ to $\theta' + \Delta\theta'/2$, where $\Delta\theta'$ was taken to be 0.1 °C.

An example of this conditional probability is shown in Figure 13. The results show that a linear relation exists between $E(w \mid \theta')$ and θ', when the data are taken at one

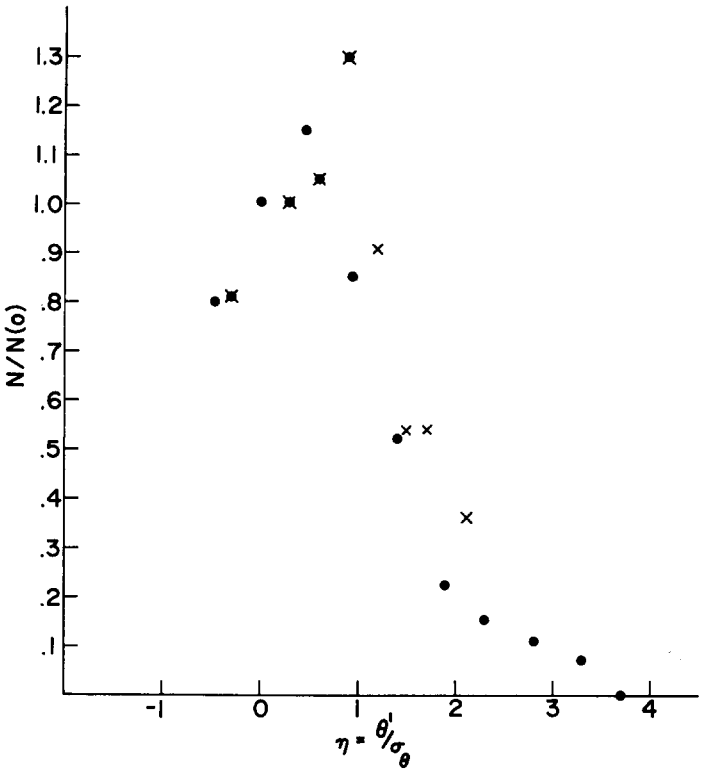

Fig. 11. Normalized population of isotherms as a function of the dimensionless temperature, η as measured from the aircraft. The normalization is the population at $\eta = 0$.

height which may be written as

$$E(w \mid \theta') = \beta\theta', \tag{43}$$

where β is a constant. It is of interest to note that $E(w/\theta') \simeq 0$ when $\theta' = 0$. Therefore the plumes are apparently defined by the $\theta' = 0$ isotherms.

The slope β is a function of height and stability. When plotted in the dimensionless form $(T_*/u_*)\,\beta$ vs. z/L it turns out that a simple almost linear relation results, (see Fig. 14) indicating that the similarity description is useful in this case.

Equation (43) indicates that the 'profiles' for temperature and vertical velocity are approximately the same when averaged over the entire plume cross-section. This is not at variance with the case study of a plume by Kaimal and Businger (1970) since no separation between the front and rear of the plumes has been made in the present analysis.

D. FURTHER CONSEQUENCES OF THE TEMPERATURE AND VELOCITY DISTRIBUTIONS

It appears that at $\theta' = 0$ approximately, the maximum number of isotherms is found (see Figure 14). If we now assume that there is a one to one correspondence between

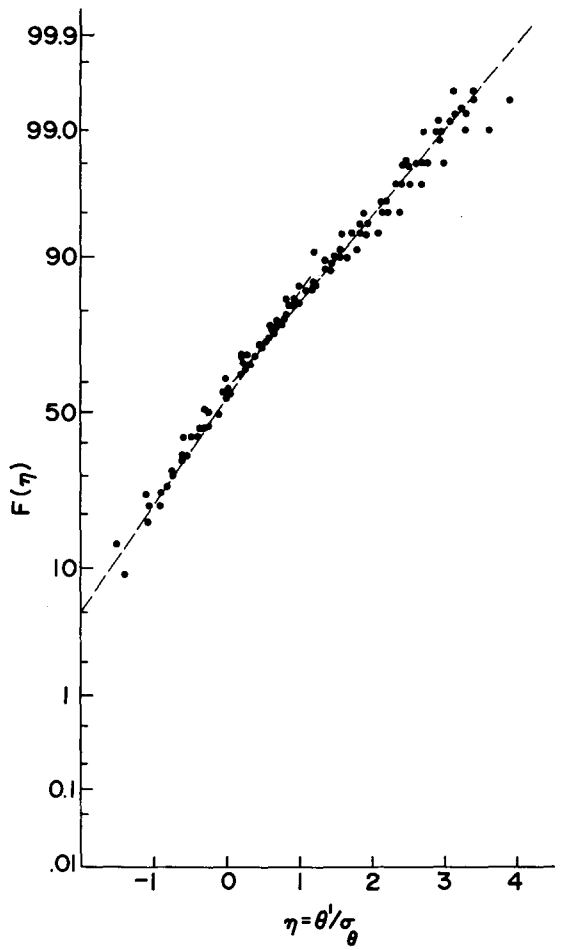

Fig. 12. Cumulative temperature distribution function vs. the dimensionless temperature η.

the number of isotherms and the number of cores (or temperature maximums), then the population of cores, $P(\theta_c')$, may be found by computing the number of isotherms that are lost in a temperature interval $d\theta'$ (or in normalized form $d\eta$).
Thus

$$P(\eta_c) = -\frac{dN}{d\eta}.$$

An estimate of the slope in Figure 14 yields the relationship $P(\eta_c) = 0.3\, N(0)$ for $\eta \leqslant 3.3$. This means that the population of cores can be represented by a uniform density distribution. We also see that the shape of the normalized distribution is independent of stability over the range of stabilities considered here. These are intriguing results which may provide stimulating information for theoretical plume models.

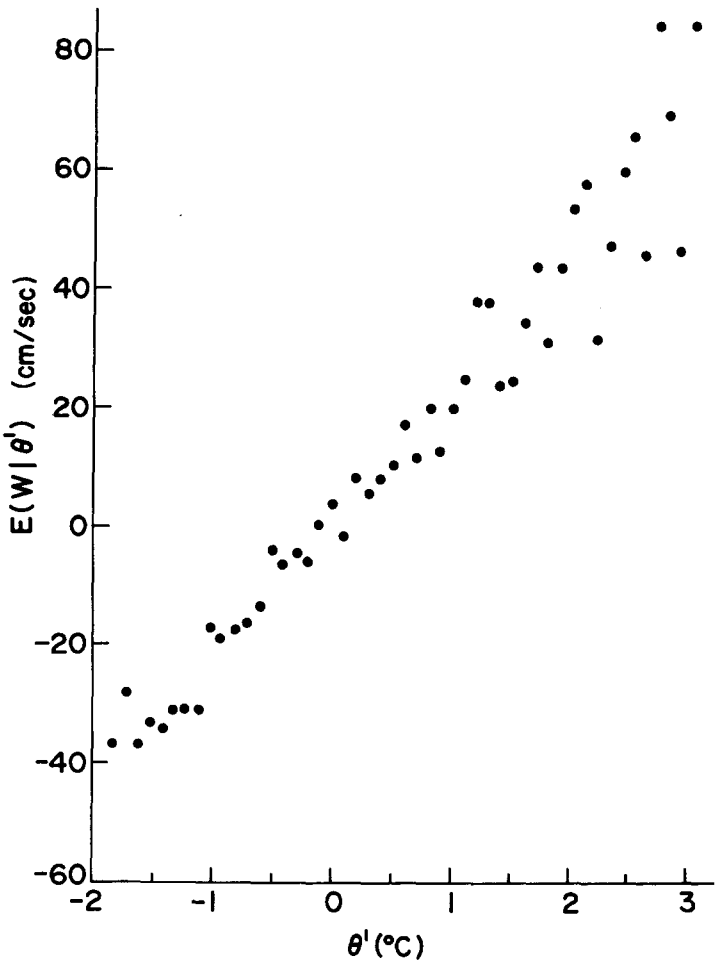

Fig. 13. Sample of conditionally expected value of w measured from the tower.

E. AVERAGE PLUME TEMPERATURE AND PLUME VERTICAL VELOCITY

The average plume temperature, $\overline{\theta}\uparrow$ was determined by integrating

$$\int_{\theta'=0}^{\theta'=\infty} \theta' \, \mathrm{d}F(\theta').$$

The results are shown in terms of $\overline{\theta}\uparrow/T^*$ in Figure 15. In addition, by use of the two temperature profiles that were available for runs 28 and 40, it was possible to determine the vertical temperature gradient inside and outside of the plumes shown in Figure 16. The results indicate that the exterior temperature is nearly adiabatic as suggested by Webb (1965).

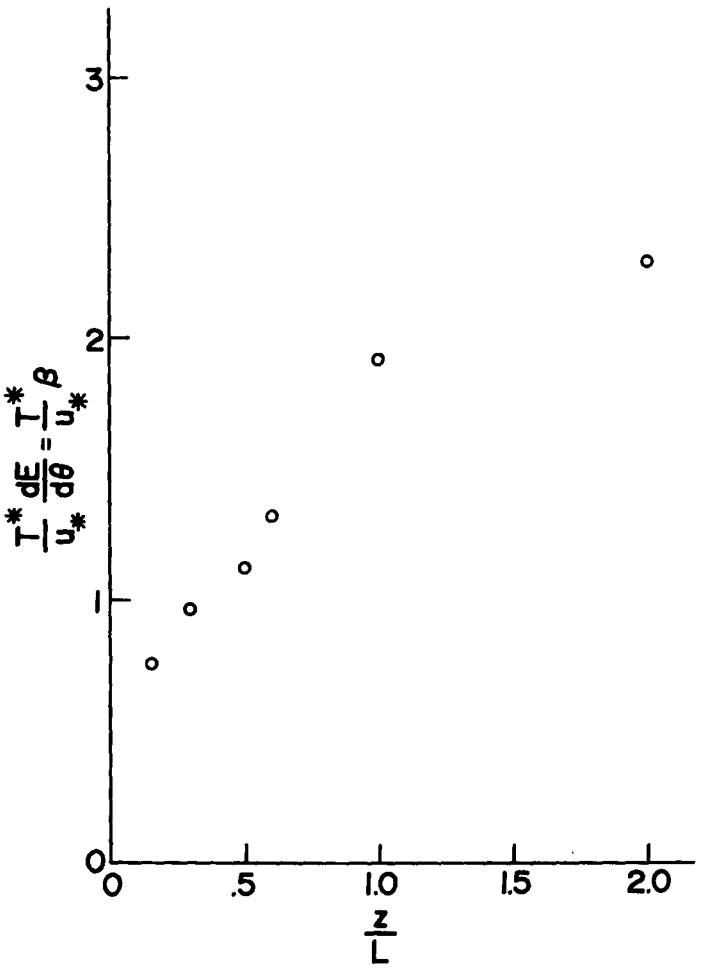

Fig. 14. Slope of the conditionally expected value of w as a function of z/L.

The average upward velocity $\bar{w}\uparrow$, at each height can be determined by taking

$$\bar{w}\uparrow = \int_{\theta'=0}^{\infty} \int_{w=-\infty}^{\infty} wf(w \mid \theta') \cdot dw \cdot f(\theta')\, d\theta',$$

where

$$f(\theta')\, d\theta = dF(\theta').$$

Now

$$\int_{w=0}^{\infty} wf(w \mid \theta')\, dw \cdot d\theta' = E(w \mid \theta') \cdot d\theta'$$

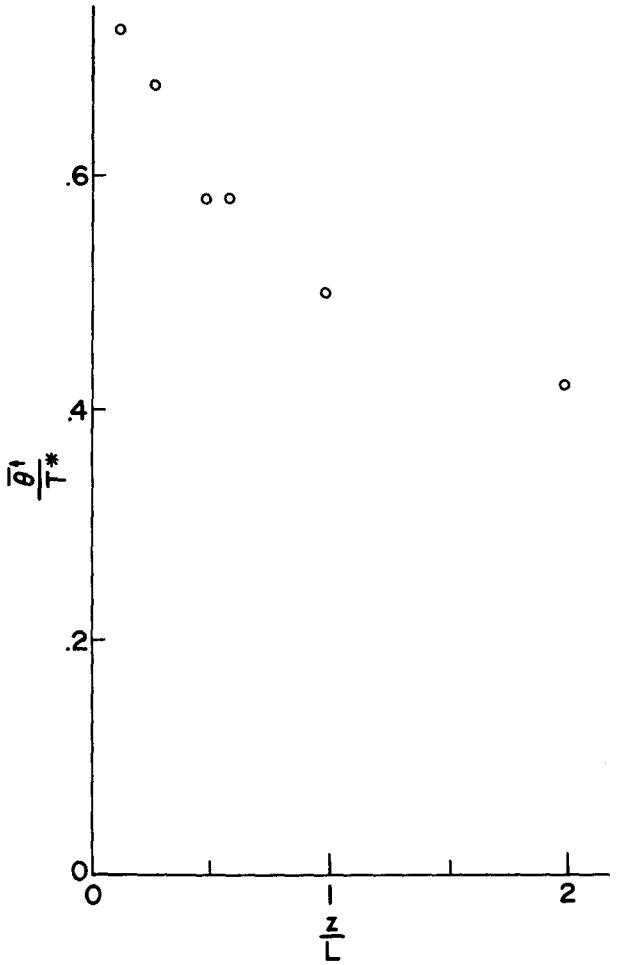

Fig. 15. Average non-dimensional plume temperature as a function of z/L.

hence

$$\bar{w}\uparrow = \int_{\theta'=0}^{\infty} E(w \mid \theta') \cdot \mathrm{d}F(\theta').$$

This average vertical velocity was determined at each height. The values are shown for two runs in Figure 17 as a function of u_* and z/L. The z dependence of $\bar{w}\uparrow$ seems to be almost proportional to z/L, from $z/L=0.2$ to $z/L=2.0$. However, since $\bar{w}\uparrow=0$ at $z=z_0$, the z dependence must be stronger than linear within the lower region. If the buoyant energy is all taken up by the divergence of the turbulent kinetic energy, then the z dependence of $\bar{w}\uparrow$ must go as $z^{1/2}$ (e.g., Bryson, 1955). Since $\bar{w}\uparrow$ increases at a rate greater than $z^{1/2}$ at $z/L>0.2$, it appears also that the pressure term must be

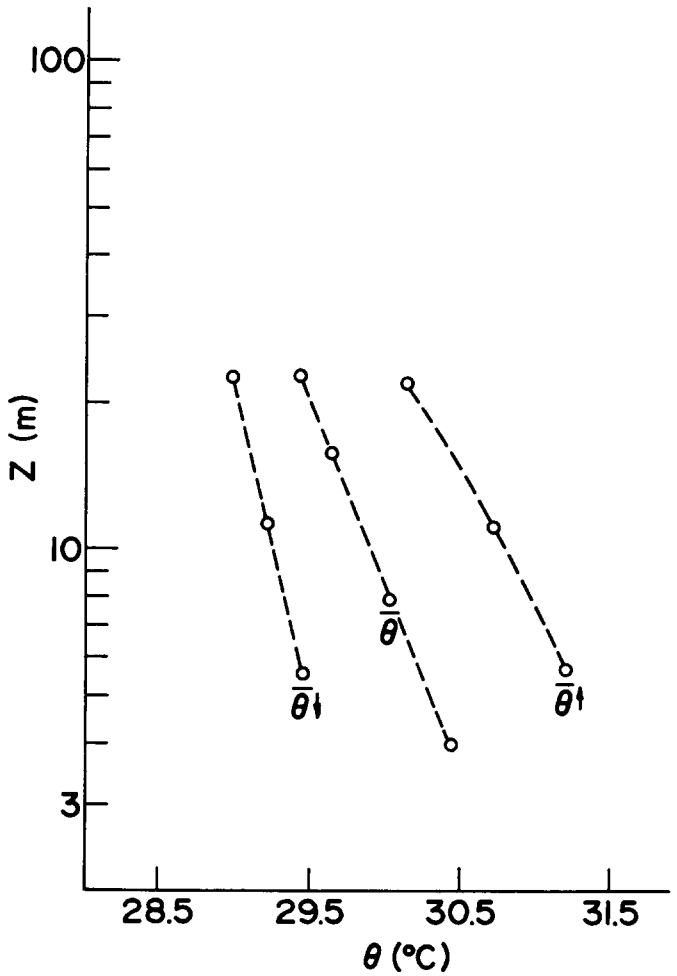

Fig. 16. Average potential temperatures vs. height for tower run 28; inside and outside the 'plume' field (dashed lines to the right and to the left, respectively) and the average (central dashed line).

important in producing this acceleration. Similar findings were reported by Kaimal and Businger (1970). These results are at odds with the model of Morton *et al.* (1956) for a neutrally stratified fluid as the dependence of w on z is an inverse power of z. However, Telford's (1966) model of an isolated plume as well as his treatment of a field of plumes (1970) does allow the air mass of the plume to accelerate upward.

5. Applications

A. HEAT FLUX

The maximum temperature is the maximum core temperature of the hottest plumes. From Figure 8, one can see $\bar{\varrho}(\eta)=0$ at $\theta' \simeq 3.6\sigma_\theta$ or the maximum temperature at

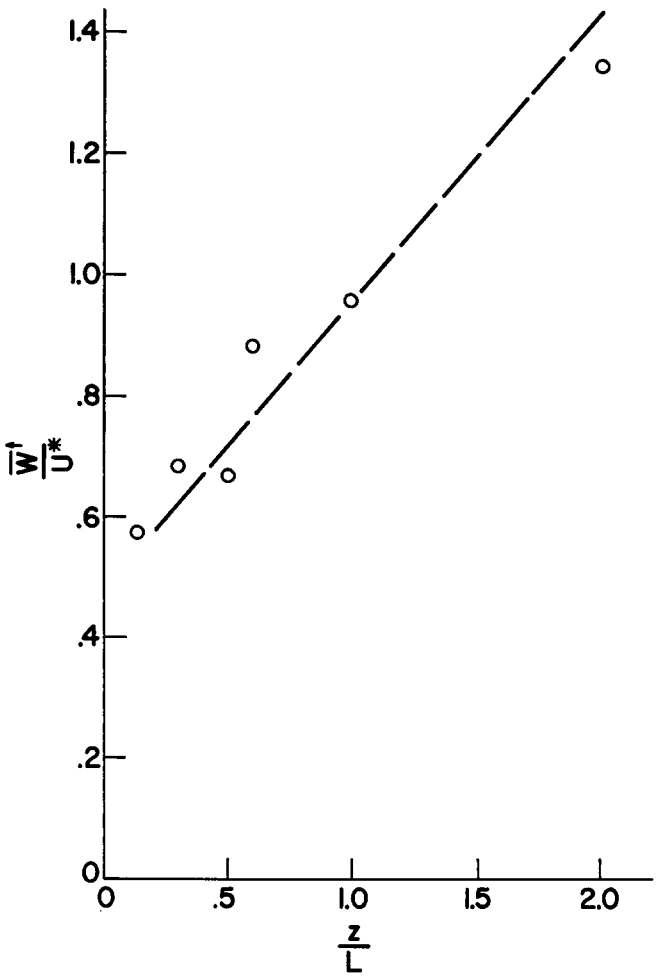

Fig. 17. Average vertical velocity of the plumes vs. z/L.

zero radius. This relation may have practical significance because $\sigma_\theta/T^* = 0.9(z/L)^{-1/3}$ for practically the whole unstable range, $z/L > 0.1$ (see Wyngaard *et al.*, 1971); thus θ'_{max} may be written

$$\theta'_{max} \simeq 3.6\, T^* \left(\frac{z}{L}\right)^{-1/3} . \tag{44}$$

This means that θ'_{max} is independent of u_* and depends on the heat flux F_h and the height as follows

$$\theta'_{max} \simeq 3.6 \left(\frac{F_h}{c_p \varrho}\right)^{2/3} \left(\frac{T}{kgz}\right)^{1/3} . \tag{45}$$

This may be a useful relation to determine the heat flux, because all that is required is a simple fast-response thermometer.

One problem is to obtain a reasonable estimate of θ'_{max} from the temperature data. From Figure 12 showing $F(\theta'/\sigma_\theta)$, $\theta'/\sigma_\theta > 3.5$ for roughly 0.5% of the time.

B. ENTRAINMENT

Using the estimate of $\bar{w}\uparrow$, since the area of the plumes is approximately constant with height $(F(0))$, the divergence of $\bar{w}\uparrow$ may be written as

$$\frac{\partial}{\partial z}\bar{w}\uparrow = \int_0^\infty \frac{\partial}{\partial z} E(w \mid \theta')\, \mathrm{d}F(\theta') = a/L, \tag{46}$$

where a is the slope of $\bar{w}\uparrow$ vs. z/L multiplied by the surface area of all of the plumes. The value of a cannot be determined yet but it is some constant. It includes the effect of merging of plumes with height. Thus the divergence of the plume field is approximately constant with height for $z/L > 0.2$. This must be accompanied by a corresponding horizontal flow into the rising air mass. For $z/L < 0.2$, the z/L dependence of w is $(z/L)^{p+1}$ where $p > 0$, and the entrainment must increase with height within this region.

These results for $z/L < 0.2$ do not agree with the assumptions of Morton *et al.* (1956) which made the divergence term proportional to the upward velocity. However, more data are needed to determine the exact form of $\bar{w}\uparrow$. Telford (1966) assumed that the entrainment rate was proportional to the rms internal turbulent velocity, and it is not possible to compare his assumption with these results.

6. Conclusion

The aircraft data indicate that for $\theta' > 0$, there are little differences in the average axes of the convective plumes measured parallel or perpendicular to the wind. However, for $\theta' < 0$, there is a suggestion of a difference, but the limited number of events over a surface with a uniform temperature, does not permit an estimate of this difference. The asymmetry of plume temperature must come from the temperature maximums being displaced from the geometric center for $\theta' > 0$. A maximum core temperature of the plume was estimated in terms of the nondimensional temperatures, by estimating the maximum value of the temperature fluctuation during the period of measurement. This gave a value of $\eta = 3.6$. Using these maximum temperatures, it was possible to relate the maximum temperature fluctuation to the heat flux.

By assuming that the vertical velocity w is composed of two terms, a temperature dependent and an independent part, the temperature dependent part was evaluated. The almost linear relationship between the temperature dependent velocity and θ' was shown to be consistent with the assumption of similar profiles between vertical velocity and temperatures for the isolated plume models. The isotherm $\theta' = 0$, has a

zero convective velocity and this isotherm was used to define the temperature reference for the part of the plume field that is moving upward.

The average velocity of the rising air appears to be proportional to z/L in the regime investigated, although the initial upward motion to the point of first measurement must be substantially greater than z/L. The average temperature of the rising part of the plumes was decreasing on the order of $(z/L)^{-1/3}$. In addition, the rate of entrainment into the upward moving plume field was estimated by examining the divergence of $\bar{w}\uparrow$, and found to be approximately constant over the range of z/L investigated.

The height where the extrapolated population of plumes goes to zero appears to be a relevant scaling height. From the present data, it appears to be independent of stability.

By computing the loss of 'isotherms' in an interval $d\eta$, the core population was found to be uniform from $\eta=0$ to $\eta=\eta_{max}$.

7. Limitations

There appear to be several problems with this type of analysis and more data are needed. The model assumes a cylindrical shape in the z direction, and the results will be modified depending upon the degree of the departure from this shape. Beran (1971) shows that inside thermal plumes under slightly unstable conditions, the velocity field may be discontinuous in the vertical for the higher velocities. If the temperature field behaves similarly, then the model for these regions should be modified. The accuracy will depend upon the ratio of the length scale of the 'hotter' air to the 'cooler' air below it. Whether similar things occur at higher heat fluxes and lower levels is still an open question.

Another problem would be irregular temperature perturbations around an approximately circular shape. This could give more intersections near the $l=0$ range and tend to overestimate the population of isotherms. The degree of error would depend on the magnitude of the perturbations with respect to the size of the circle.

Acknowledgments

The authors are especially grateful to Dr. Duane Haugen and his coworkers at AFCRL for making available the data from the Kansas tower used in this study. The research has been supported in part by NSF grants GA-14680 and GA-31317X. Furthermore the senior author expresses his appreciation for the many helpful discussions he had with Dr. R. A. Shorack as well as the help he received with the writing from Elaine Mally.

List of Symbols

Symbol	*Definition*
a, b	axes of elliptical isotherms with temperature θ'
c_p	specific heat of air at constant pressure

D	acceleration depth (see Section 4b)
$f(\varrho(\eta'), \eta_c)$	a joint density distribution function
$f_{1,\theta'}(b)$	probability density functions characterizing the two axes (a and b) of the population of elliptical isotherms with temperature θ'
F_h	the turbulent heat flux (mw cm^{-2})
$F(\eta)$	cumulative distribution function of the non-dimensional temperature $\eta = \theta'/\sigma_\theta$
g	acceleration of gravity
k	von Karman's constant
$L \equiv +\dfrac{\varrho c_p \theta u_*^3}{kgF_h}$	the Obukhov length†
l_x	chord lengths intersected in the x direction with ellipses of temperature θ'
l_y	chord lengths intersected in the y direction with ellipses of temperature θ'
$m_0 = a/b$	ratio of elliptical axes
$n_{\theta'}$	number of intersections
$N(\theta')$	number of isotherms per unit area with temperature θ'
$Ri = \dfrac{g(\partial\theta/\partial z)}{\theta(\partial u/\partial z)^2}$	Richardson number
$T^* \equiv \dfrac{F_h}{ku_*\varrho c_p}$	a scaling temperature
U	average wind velocity
u_*	friction velocity
w	vertical velocity
w'	vertical turbulent velocity
$w_c(\theta')$	the convective vertical velocity
$w_{x,\theta'}(l_y \mid a)$	conditional probability density functions for chord length l_x for temperature θ' from ellipses with axis a
$w_{y,\theta'}(l_y \mid b)$	conditional probability density functions for chord lengths l_y for temperature θ' from ellipses with axis b
z	height above the ground
β	coefficient of thermal expansion
$\eta \equiv \theta'/\sigma_\theta$	a nondimensional temperature
θ	potential temperature
θ_{ref}	reference temperature
θ'	fluctuating part of the potential temperature
κ	thermal diffusivity

† Because our study deals exclusively with unstable conditions, the customary minus sign has been omitted in our definition of L.

ν	kinematic viscosity
ϱ	air density
$\varrho(\eta) \equiv \frac{\bar{a}(\eta)}{D^{2/3}L^{1/3}}[\log_{10}(D/z)+1.3]$	an average nondimensional radius of the isotherms
$\sigma_\theta \equiv (\theta'^2)^{1/2}$	rms of temperature fluctuations

References

Bean, B. R., Gilmer, R., Grossman, R. L., McGavin, R., and Travis, C.: 1972, 'An Analysis of Airborne Measurements of Vertical Water Vapor Flux during Bomex', submitted to *J. Atmospheric Sci.*

Beran, D. W.: 1971, 'Acoustic Radar Detection Techniques', *FAA Turbulence Symposium.*

Bryson, Reid A.: 1955, 'Convective Transfer with Light Winds', *Trans. Am. Geophys. Union* **36**, 209.

Businger, J. A., Wijngaard, J. C., Izumi, Y., and Bradley, E. F.: 1971, 'Flux-Profile Relationships in the Atmospheric Surface Layer', *J. Atmospheric Sci.* **28**, 181–189.

Chandra, K.: 1938, 'Instability of Fluids Heated from Below', *Proc. Roy. Soc.* **A164**, 231.

Haugen, D. A., Kaimal, J. C., and Bradley, E. F.: 1971, 'An Experimental Study of Reynolds Stress and Heat Flux in the Atmospheric Surface Layer', *Quart. J. Roy. Meteorol. Soc.* **97**, 168–180.

Kaimal, J. C. and Haugen, D. A.: 1967, 'Characteristics of Vertical Velocity Fluctuation Observed on a 430 m Tower', *Quart. J. Roy. Meteorol. Soc.* **93**, 305–317.

Kaimal, J. C. and Businger, J. A.: 1970, 'Case Studies of a Convective Plume and a Dust Devil', *J. Appl. Meteorol.* **9**, 602–620.

Lenschow, D. H.: 1970, 'Airplane Measurements of Planetary Boundary Layer Structure', *J. Appl. Meteorol.* **9**, 874–884.

McAllister, L. G., Pollard, J. R., Mahoney, A. R., and Shaw, P. J. R.: 1969, 'Acoustic Sounding – A New Approach to the Study of Atmospheric Structure', *Proc. IEEE* **57**, 579–587.

McBean, G. A., Stewart, R. W., and Miyake, M.: 1971, 'The Turbulent Energy Budget near the Surface', *J. Geophys. Res.* **76**, 6540–6549.

Monin, A. S. and Yaglom, A. M.: 1971, *Statistical Fluid Mechanics* **1**, MIT Press, Cambridge, Mass.

Morton, B. R., Taylor, G. I., and Turner, J. W.: 1956, 'Turbulent Gravitational Convection from Maintained and Instantaneous Sources', *Proc. Roy. Soc. London* **A234**, 1–23.

Morton, B. R.: 1957, 'Buoyant Plumes in a Moist Atmosphere', *J. Fluid Mech.* **2**, 127–144.

Obukhov, A. M.: 1946, 'Turbulence in an Atmosphere with a Non-Uniform Temperature', *Trudy Inst. Teoret. Geofis. AN SSSR*, No. 1. (Translation in: *Boundary-Layer Meteorol.* **2**, 7–29).

Priestley, C. H. B., 1954, 'Vertical Heat Transfer from Impressed Temperature Fluctuations', *Australian J. Phys.* **7**, 202–209.

Priestley, C. H. B.: 1956, 'Convection from the Earth's Surface', *Proc. Roy. Soc. London,* **A238**, 287–304.

Priestley, C. H. B. and Ball, F. K.: 1955, 'Continuous Convection from an Isolated Source of Heat', *Quart. J. Roy. Meteorol. Soc.* **81**, 144–157.

Taylor, R. J.: 1958, 'Thermal Structures in the Lowest Layers of the Atmosphere', *Australian J. Phys.* **11**, 168–176.

Taylor, R. J., Warner, J., and Bacon, N. E.: 1970, 'Scale Length in Atmospheric Turbulence as Measured from an Aircraft', *Quart. J. Roy. Meteorol. Soc.* **96**, 750–755.

Telford, J. W.: 1966, 'The Convective Mechanism in Clear Air', *J. Atmospheric Sci.* **23**, 652–666.

Telford, J. W.: 1970, 'Convective Plumes in a Convective Field', *J. Atmospheric Sci.* **27**, 347–358.

Telford, J. W. and Warner, J.: 1967, 'Convection Below Cloud Base', *J. Atmospheric Sci.* **24**, 374–382.

Turner, J. S.: 1963, 'The Motion of Buoyant Elements in Turbulent Surroundings', *J. Fluid Mech.* **16**, 1–16.

Vulf'son, N. I.: 1961, *Convective Motions in a Free Atmosphere*, Israel Program for Scientific Translations, Jerusalem (translated 1964). Clearing house, U.S. Dept. of Commerce. π64–11017, 188 pp.

Webb, E. K.: 1965, 'Aerial Microclimate', *Meteorol. Monographs* **6**, 27–58.

Woodward, Betsy: 1959, 'The Motion in and Around Isolated Thermals', *Quart. J. Roy. Meteorol. Soc.* **85**, 144–151.

Wyngaard, J. C., Coté, O. R., and Izumi, Y.: 1971, 'Local Free Convection, Similarity, and the Budgets of Shear Stress and Heat Flux', *J. Atmospheric Sci.* **28**, 1171–1182.